

# Software development and its description for Geoid determination based on Spherical-Cap-Harmonics Modelling using digital-zenith camera and gravimetric measurements hybrid data

**K Morozova<sup>1,2</sup>, R Jaeger<sup>3</sup>, J Balodis<sup>2</sup> and J Kaminskis<sup>1</sup>**

<sup>1</sup>Riga Technical University, Faculty of Building and Civil Engineering, Kipsalas street 6A, LV-1048, Riga, Latvia

<sup>2</sup>University of Latvia, Institute of Geodesy and Geoinformatics, Boulevard of Rainis 19, LV-1586, Riga, Latvia

<sup>3</sup>Hochschule Karlsruhe – University of Applied Sciences, Institute of Applied Research, Moltkestrasse 30, 76133, Karlsruhe, Germany

E-mail: katerina.morozova@edu.rtu.lv

**Abstract.** Over several years the Institute of Geodesy and Geoinformatics (GGI) was engaged in the design and development of a digital zenith camera. At the moment the camera developments are finished and tests by field measurements are done. In order to check these data and to use them for geoid model determination DFHRS (Digital Finite element Height reference surface (HRS)) v4.3. software is used. It is based on parametric modelling of the HRS as a continuous polynomial surface. The HRS, providing the local Geoid height  $N$ , is a necessary geodetic infrastructure for a GNSS-based determination of physical heights  $H$  from ellipsoidal GNSS heights  $h$ , by  $H=h-N$ . The research and this publication is dealing with the inclusion of the data of observed vertical deflections from digital zenith camera into the mathematical model of the DFHRS approach and software v4.3. A first target was to test out and validate the mathematical model and software, using additionally real data of the above mentioned zenith camera observations of deflections of the vertical. A second concern of the research was to analyze the results and the improvement of the Latvian quasi-geoid computation compared to the previous version HRS computed without zenith camera based deflections of the vertical. The further development of the mathematical model and software concerns the use of spherical-cap-harmonics as the designed carrier function for the DFHRS v.5. It enables - in the sense of the strict integrated geodesy approach, holding also for geodetic network adjustment - both a full gravity field and a geoid and quasi-geoid determination. In addition, it allows the inclusion of gravimetric measurements, together with deflections of the vertical from digital-zenith cameras, and all other types of observations. The theoretical description of the updated version of DFHRS software and methods are discussed in this publication.

## 1. Introduction

The DFHRS software has been developed at Karlsruhe University of Applied Sciences, Institute of Applied Research for the computation of precise quasi-geoid models from different kind of data starting in 1999 [1]. The computation of precise quasi-geoid models, providing the local quasi-geoid height  $N(B,L,h)$  as a function of the position in terms of the ellipsoidal geographical coordinates  $(B,L,h)$ , plays

a significant role as geodetic infrastructure in the age of precise GNSS positioning technologies, in respect to transform by  $H=h-N$  an ellipsoidal GNSS height  $h$  into the physical normal height  $H$ . The GNSS based determination of physical heights  $H$  is much faster, easier to handle and much more economic, in comparison to classical geodetic levelling. The principle of the DFHBF-approach and software version 4.3 (v. 4.3) [1] is based on the parametric model of  $N(B,L,h)$  as a continuous polynomial height reference surface (HRS). The access to the parametric HRS model is enabled by DFHRS\_DB data-bases and access-software, which allow the direct conversion of GNSS-heights  $h$  into physical standard heights  $H$  by  $H=h-N$ . The DFHBF\_DB stores polynomial  $p$  parameters and (a scale-difference factor  $\Delta m$  for old height  $H$  systems) [1],[2]. DFHRS v4.3 includes all types of geometrical input data: Both ellipsoidal heights  $h$ , and normal/orthometric heights  $H$ , geoid/Q-geoid-heights  $N$ , and deflections of the vertical ( $\eta, \zeta$ ) out of geopotential models (EGM2008) or grids. The updated software v4.3 includes observed vertical deflections data ( $\eta, \zeta$ ) from digital zenith cameras [3]. The region of Riga is chosen for tests of the camera system, data modelling tests and data quality analysis in this publicaion.

## 2. Used data

The Riga region as test area includes 35 GNSS /levelling points ( $h,H$ ) and 10 deflections of the vertical data points ( $\eta, \zeta$ ) observed by the developed digital zenith camera. This observation data were commenced in September, 2016 and will be continued in order to cover the whole territory of Latvia. The GNSS observations were partially provided by Latvian Geospatial Information Agency, as well as being carried out in 4 hours sessions and processed by GGI stuff using Bernese GNSS software v 5.2. Besides field data observations from the developed zenith camera and GNSS/levelling points, quasi-geoid data  $N$  and vertical deflections data ( $\eta, \zeta$ ) were derived from EGM2008 and EIGEN6C4 geopotential models <http://icgem.gfz-potsdam.de/ICGEM/> [4]. Both models are of the same degree and order  $n=m=2159$ .

The graphical display of the polynomial mesh (thin blue lines) and patch design (thick blue lines) and the observed data (fitting points and deflections of the vertical) of the DFHBF software 4.3 are depicted in figure 1.

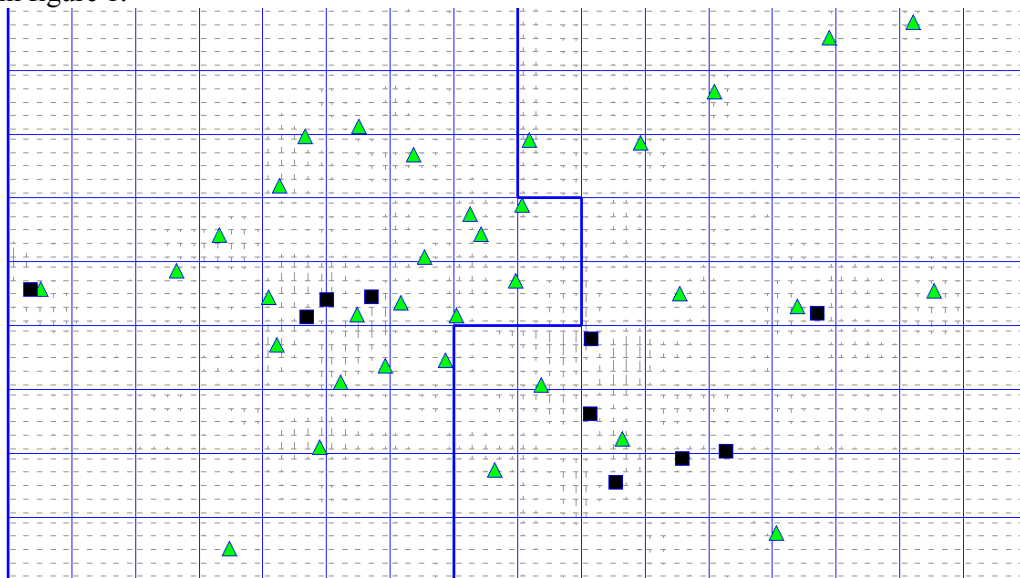


**Figure 1.** Riga region observations (green triangles – GNSS/levelling points, black squares – deflections of the vertical).

### 3. Deflections of the vertical

The astronomic latitude  $\Phi$  and longitude  $\Lambda$  determine the direction of the tangent to the plumb line, and the geodetic coordinates  $(B,L)=(\varphi, \lambda)_{\text{ell}}$  define the direction of the ellipsoid normal [5]. The deflections of the vertical  $(\eta, \zeta)$  measured at the earth surface are the angular difference between plumb line direction and normal to the surface and consists of north and east component [6]. The use of observations  $(\eta, \zeta)$  from digital zenith camera allows to compute quasi-geoid models  $N$  using (6a-d) with much less GNSS/levelling points in a given area. Figure 2 shows the observation type of vertical deflections and its components, here related to the sphere, while the surface observations are by (6a-d) related to the ellipsoidal latitude and longitude  $(B, L)$ . The relationship of unreduced deflections related to the Earth surface, and the quasi-geoid is shown in figure 3. Deflections of the vertical measured at the Earth surface by means of a digital zenith camera in North-South and East-West direction can be calculated by the difference of astronomical and ellipsoidal coordinates, determined by GNSS, as follows:

$$\xi = \Phi - B$$

$$\eta = (\Lambda - L)\cos\varphi$$

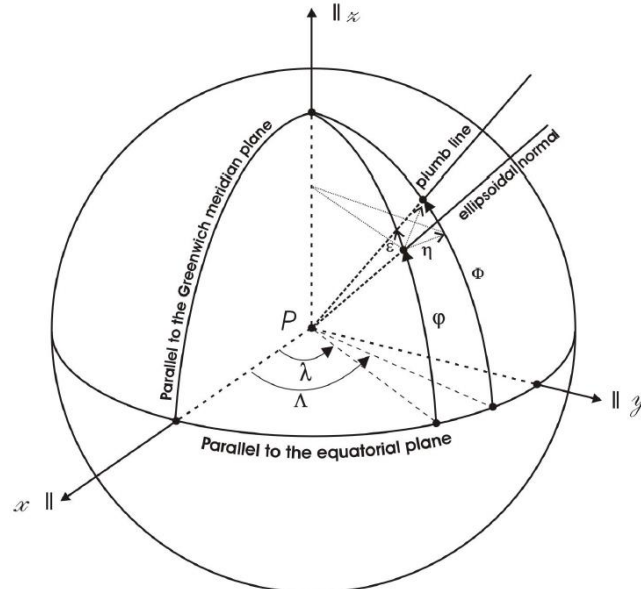


Figure 2. Vertical deflections  $(\eta, \zeta)$ , here related to the sphere, and its components. [6]

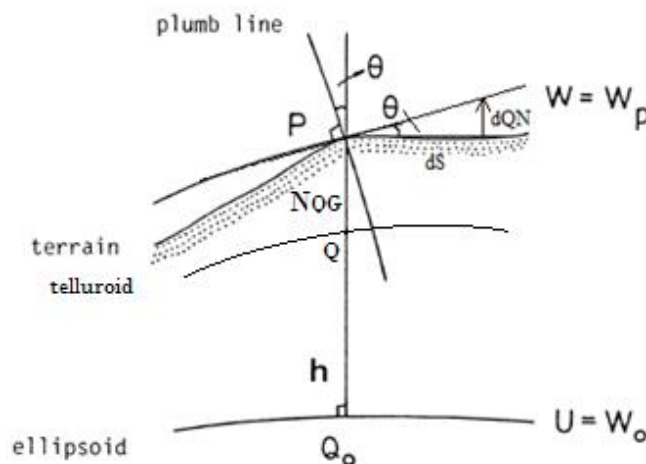


Figure 3. The relationship of unreduced deflections of vertical related to the Earth surface and the quasi-geoid

#### 4. Digital Zenith camera

The digital zenith camera system has been developed in the recent years by the University of Latvia, Institute of Geodesy and Geoinformatics [7], [8]. At present the camera system developments have been completed, and first observations are done in the region of Riga. The instrument consists of vertically oriented telescope, equipped with sensitive tiltmeter; assembly can be rotated around vertical axis. The tiltmeter readings provide inclination corrections for the instrument main axis relative to the plumb line. The principle of digital zenith camera is based on the determination of plumb line by astronomical coordinates  $(\Phi, \Lambda)$ . The stars serve as orientation and approximately 20 stars around zenith frame should be used as observations. The precision of the developed digital zenith camera is about 0,1-0,2 arc seconds. The advantage of using deflections of the vertical observations is the provision of terrestrial gravity field information, which is independent from errors in local vertical datum [9], [10]. GNSS techniques allow to determine geodetic (ellipsoidal) coordinates  $(B,L)=:(\varphi, \lambda)_{\text{ell}}$  (see 6a,b), as well as the exact time of positioning, which is needed for the astronomical zenith camera observations  $(\Phi, \Lambda)$  for the modelling of the precession, nutation and Earth rotation terms.

#### 5. Results

Different computation results are depicted in figure 4, figure 5 and figure 6. Figure 4 shows the difference of the quasi-geoid models N based on EGM2008 and EIGEN6C4 geopotential models. In most parts of Riga region the amplitude of difference in geoid heights is in range from -1 up to +1 cm. The difference in the north of Riga region can reach up to 3 cm. The figure 5 depicts the use of deflections of vertical data derived from EGM2008 model and its impact on geoid heights determination. This difference can reach from -3 up to +3 cm. Figure 6 shows the differences of deflections of vertical observations from digital zenith camera in comparison without using this data. The range of differences varies from -7 up to +5 cm, what proves significant impact and improvement of the use of deflections of the vertical  $(\eta, \xi)$  on a quasi-geoid determination. The standard deviation of the deflections of vertical data is equal to 0,09 arcsec for  $\xi$  (North- South) component and 0,14 arcsec for  $\eta$  (East-West) component. Other statistics is performed in table 1.

**Table 1.** Statistics of vertical deflections observations

|        | Mean  | RMS  | Min    | Max   |
|--------|-------|------|--------|-------|
| $\xi$  | 0,072 | 0,09 | -0,100 | 0,162 |
| $\eta$ | 0,091 | 0,14 | -0,311 | 0,226 |

The calculations based on the preliminary results of vertical deflections observations approve the successful use of digital zenith camera and instrument readiness for further collection of observations. The computations using the DFHRS software v.4.3 allowed to carry out additional control and software's check for modelling and data errors in the frame of the data processing.

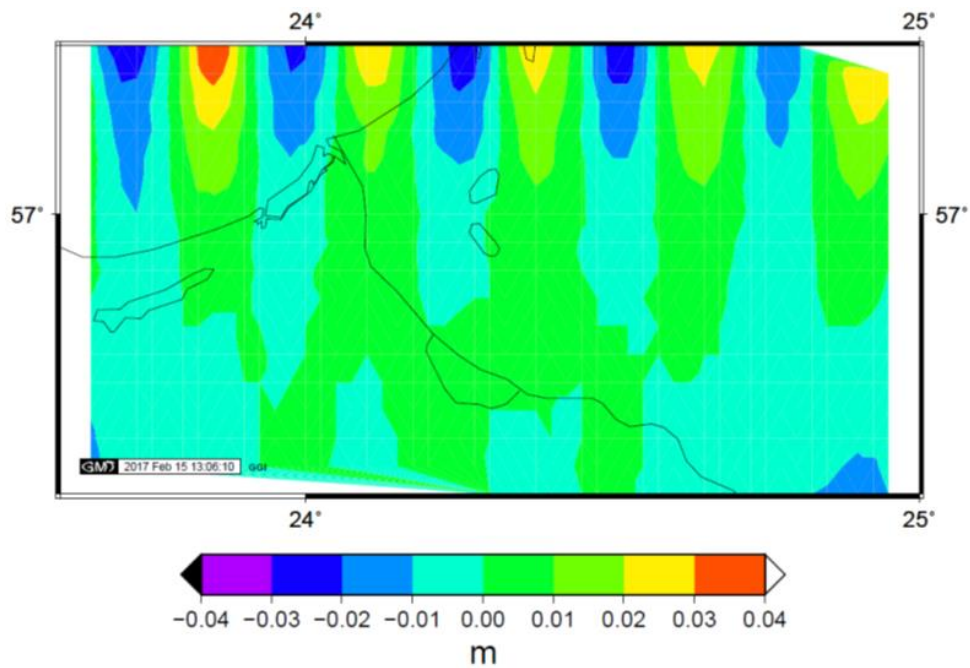


**Figure 4.** The difference of quasi-geoid model for Riga region in comparison to EIGEN6C4 and EGM2008 geopotential models.

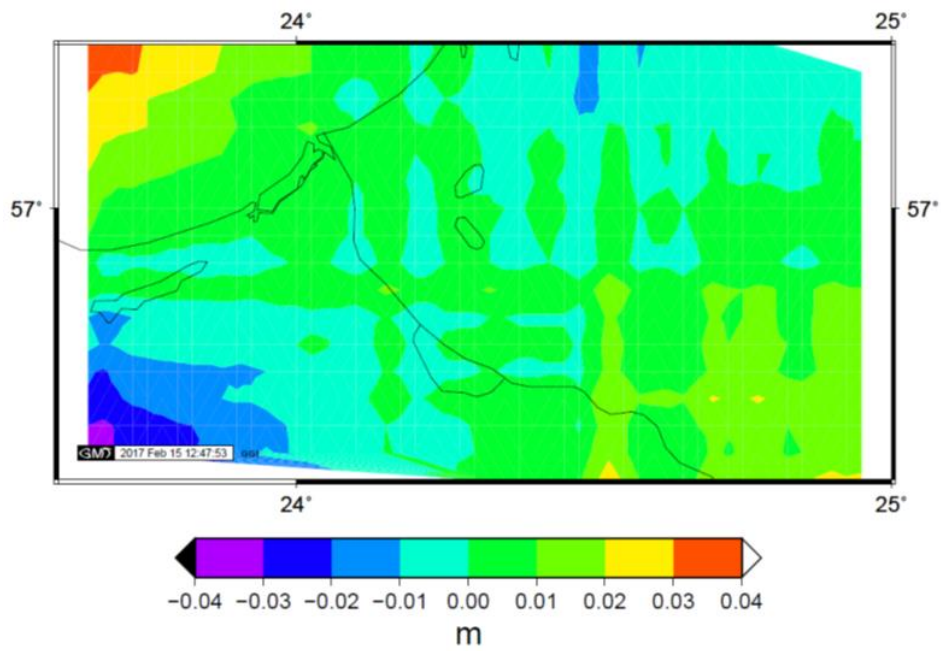


**Figure 5.** The difference between using derived deflections of vertical data and without this data.

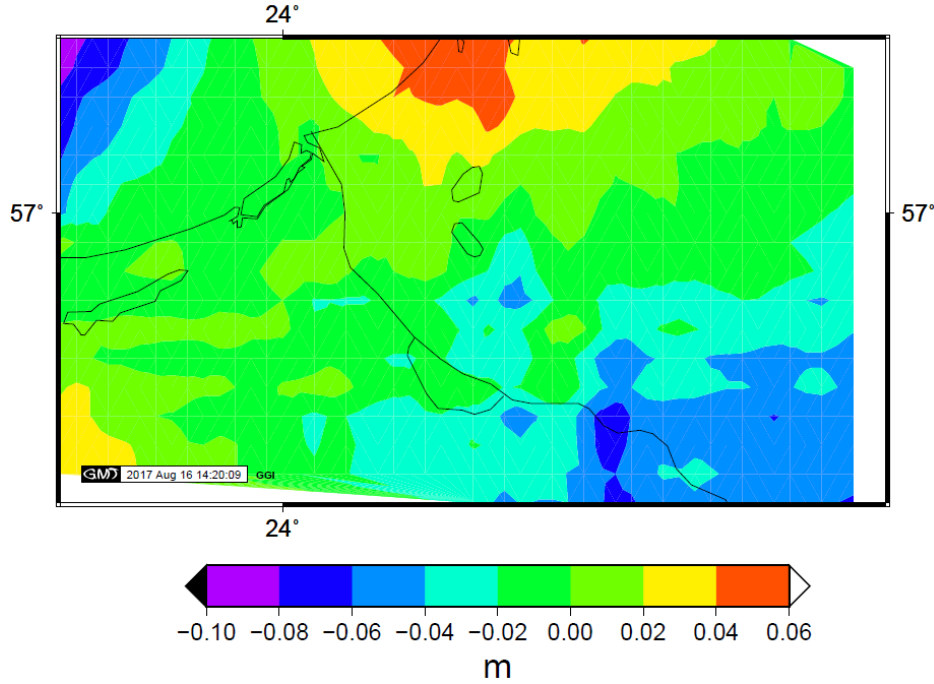


**Figure 6.** The impact of vertical deflections data from digital zenith camera.

## 6. Further development of the software

The further development of the software concerns the use of spherical-cap-harmonics as the designed carrier function for the DFHRS v.5.1. It enables - in the sense of the strict integrated geodesy approach, holding also for geodetic network adjustment - both a full gravity field and geoid determination. In addition it allows the inclusion of gravimetric measurements, together with deflections of the vertical from digital zenith cameras, and all the other types of observations. The advantage of spherical-cap-harmonics (SCH) modelling in comparison to spherical harmonics (SH) that less parameters are needed in order to compute local area instead of whole sphere. [11], [12]. This method was developed by [13], [14]. The gravitational potential  $V$  in terms of SCH for a point  $P(r, \alpha, \theta)$  within the cap reads [15]:

$$V(r, \alpha, \theta) = \frac{GM}{R} \sum_{k=0}^{k \max} \left(\frac{R}{r}\right)^{n(k)} \sum_{m=0}^k (C'_{nm} \cos m\alpha + S'_{nm} \sin m\alpha) \bar{P}_{n(k),m}(\cos\theta) \quad (1)$$

The  $C'_{nm}$  and  $S'_{nm}$  coefficients are unknowns and have to be determined by least square estimation.

The basic concept behind SCH is to expand gravity potential  $V$  in two sets of basis functions which satisfies Laplace's equation [16], [17] within the spherical cap and are mutually orthogonal in each set. The Legendre functions are chosen in order to satisfy the following boundary conditions [13]:

$$\frac{dP_{n_k}^m(\theta=\alpha)}{d\theta} = 0 \text{ for } k - m = \text{even}, \quad (2)$$

$$dP_{n_k}^m(\theta = \alpha) = 0 \text{ for } k - m = \text{odd}, \quad (3)$$

where  $\alpha$  is the cap half-angle, and  $k$  is used to index (in ascending order) the roots  $n_k$  of (2) and (3) at a given value of  $m$  [18].

The local coordinate system is defined by cap opening angle and local pole is depicted on figure 7.

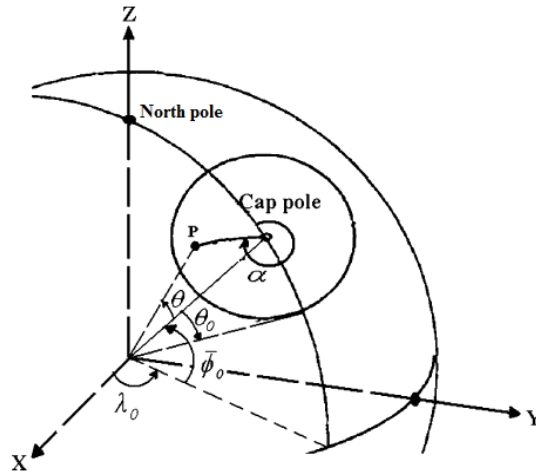


**Figure 7.** Spherical cap area with its own pole located at the origin of area of interest [12]

The starting point for the Quasi-Geoid based theory of Molodensky implemented in the DFHRS-approach and software 5.0 reads with:

$$T_P = (V(r, \alpha, \theta | C'_{nm}, S'_{nm}) + Z(x, y, z) - U(\beta, \alpha, u))_P \quad (4a)$$

$$N_{QG} = \frac{(V + Z - U)_P}{\gamma_Q} = \frac{T_P}{\gamma_Q} \quad (4b)$$

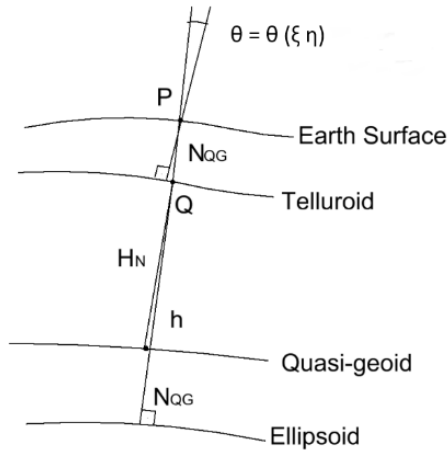


**Figure 8.** Deflection of vertical at point P

Consistent with the above Quasi-Geoid theory of Molodensky and the Bruns theorem, we have zenith-camera based measured surface vertical deflections at surface point P, referring to the telluroid point Q (see figure 8):

$$\xi_P = \varphi_{astr,P} - B \quad (6a)$$

$$\eta_P = (\alpha_{astr,P} - L) * \cos B \quad (6b)$$

Starting with the Quasi-Geoid formula and introducing again the potential model related  $T_P$  we get the vertical deflections at the Earth Surface P as (see figure 8.)

$$\begin{aligned}\xi_P &= -\frac{dN_{QG}}{ds_{North}} = -\frac{\partial N_{QG}}{\partial B} \frac{\partial B}{\partial s_N} = -\frac{\partial B}{\partial s} \frac{\partial N_{QG}}{\partial B} = \frac{-1}{(M+h)} \frac{1}{\gamma_Q} \frac{\partial}{\partial B} T_P \\ &= \frac{-1}{\gamma_Q(M+h)} \left(\frac{\partial T}{\partial B}\right)_P + \delta\xi_{norm.curv.} \quad (6c)\end{aligned}$$

$$\eta_P = -\frac{dN_{QG}}{ds_{East}} = -\frac{\partial L}{\partial s} \frac{\partial N_{QG}}{\partial L} = \frac{-1}{(N+h)\cos B} \frac{1}{\gamma_Q} \frac{\partial}{\partial L} T_P = \frac{-1}{\gamma_Q(N+h)\cos B} \left(\frac{\partial T}{\partial L}\right)_P \quad (6d)$$

$\delta\xi_{norm.curv.}$  is the difference between Helmert and Molodensky deflections due to the curvature of the normal plumb line [19].

For above differentiation of  $T_P$  in the direction of the ellipsoidal latitude  $B$  and longitude  $L$  4 different coordinate systems in  $T_P$  have to be handled, as we have (4), the solution at first we bring together the local CAP system and the spherical system, we have:

$$r = r \quad (7a)$$

$$\tan\alpha = \frac{\cos\varphi\sin(\lambda - \lambda_0)}{\sin\varphi\cos\varphi_0 - \cos\varphi\sin\varphi_0\cos(\lambda - \lambda_0)} \quad (7b)$$

$$\cos\theta = \sin\varphi\sin\varphi_0 - \cos\varphi\cos\varphi_0\cos(\lambda - \lambda_0) \quad (7c)$$

For the remaining 3 systems for the position of the point  $P$ , the common denominator are the Cartesian 3D coordinates  $(x,y,z)$ :

$$\begin{bmatrix} x \\ y \\ z \end{bmatrix} = \begin{bmatrix} r\cos\varphi\cos\lambda \\ r\cos\varphi\sin\lambda \\ r\sin\varphi \end{bmatrix} \quad (8)$$

$$\begin{bmatrix} x \\ y \\ z \end{bmatrix} = \begin{bmatrix} (N(B) + h)\cos(B)\cos(L) \\ N(B) + h)\cos(B)\sin(L) \\ \left(\frac{b^2}{a^2}N(B) + h\right)\sin(B) \end{bmatrix} \quad (9)$$

$$\begin{bmatrix} x \\ y \\ z \end{bmatrix} = \begin{bmatrix} u\sqrt{1 + \varepsilon^2/u^2} \cos\beta\cos\lambda \\ u\sqrt{1 + \varepsilon^2/u^2} \cos\beta\sin\lambda \\ u\sin\beta \end{bmatrix} \quad (10)$$

With (7a, b, c), (8), (9) and (10) and the common relation to  $(x, y, z)$  we have consistency in the georeferencing and we can set up the derivatives  $\left(\frac{\partial T}{\partial B}\right)_P$  (6a) and  $\left(\frac{\partial T}{\partial L}\right)_P$  (6b) by applying the chain rule to (7a, b, c) to (10) using MAPLE.

So the vertical deflections parametrize now in DFHRS 5.x the carrier function of the spherical Cap harmonics potential and respective  $C_{nm}$ ,  $S_{nm}$  coefficients instead of polynomial coefficients used in the DFHRS approach and software 4.x. By DFHRS 5.x also surface gravity measurements  $g_P$  can be included, in opposite the DFHRS 4.x.

From the final potential computed in a least squared adjustment the Q-Geoid can be computed again by using (4) and (4a). A geoid can be computed afterward by applying:

$$N_G = N_{QG} + \frac{\bar{g} - \bar{\gamma}}{\bar{\gamma}} H \quad (11)$$

## 7. Conclusions

The method of spherical-cap-harmonics modelling in terms of integrated geodesy allows to compute precise quasi-geoid model to be used for GNSS measurements. Combination of all data gives an opportunity to define height reference surface using independent measurements (both geometrical and



physical observations). The use of vertical deflections measurements allow to check/control reliability of heights computed by GNSS/levelling points. SCH in comparison to ordinary SH is fast method and does not need so much memory for computations [20], [21]. The realization of this method combining all data and implementation in DFHRS v 5.0 version will be developed under Visual Studio 2015 using C++ programming language.

### Acknowledgments

The research was developed during ERASMUS+ traineeship in Hochschule Karlsruhe – University of Applied Sciences under supervision of Prof. Dr.-Ing. Reiner Jäger. Thanks to Institute of Geodesy and Geoinformatics for provided digital zenith camera data and Latvian Geospatial Information Agency for provided GNSS/levelling data.

### References

- [1] Jäger R 2000-2017 DFHBF-Website, <http://dfhbf.de/>
- [2] Jäger R, Kaminskis J, Strauhmanis J and Younis G 2012 Determination of quasi-geoid as height component of the geodetic infrastructure for GNSS positioning services in the Baltic States *Latvian J. of Physics and Technical Sciences* **3** 5–15
- [3] Owusu-Banahene W 2013 Further development of the DFHRS concept and software (C++) under Visual Studio 2012 and computation of the Geoid for Albania. Master's thesis *University of Applied Sciences*
- [4] International Center for Global Earth Models (ICGEM) website, <http://icgem.gfz-potsdam.de/ICGEM/>
- [5] Halicioglu K, Deniz R and Ozener H 2012 Digital zenith camera system for Astro-Geodetic applications in Turkey, *Journal of Geodesy and Geoinformation, Chamber of Surveying and Cadastre Engineers vol. 1, Issue 2, Journal No. 106* Doi: 10.9733/jgg.131212.1 p [115-120].
- [6] Ceylan A. 2009 Determination of the deflection of vertical components via GPS and levelling measurement: A case study of a GPS test network in Konya, Turkey, *Scientific research and essay Vol. 4, (12)*, pp. 1438-1444
- [7] Zariņš A, Rubans A and Silabriedis G 2016 Digital zenith camera of the University of Latvia, *Geodesy and Cartography*, **42:4**, 129-135 <http://dx.doi.org/10.3846/20296991.2016.1268434>
- [8] Abele M, Balodis J, Janpaule I, Lasmane I, Rubans A and Zariņš A. 2012 Digital zenith camera for vertical deflection determination, *Geodesy and Cartography* **38**: 123–129. <https://doi.org/10.3846/20296991.2012.755324>
- [9] Featherstone W E and Lichten D D 2008 Fitting gravimetric geoid models to vertical deflections, *Journal of Geodesy* **83**(6):583-589, DOI: 10.1007/s00190-008-0263-4
- [10] Voigt C, Denker H and Hirt C 2009 Regional Astrogeodetic Validation of GPS/Levelling Data and Quasigeoid Models. In: Sideris M.G. (eds) Observing our Changing Earth. *International Association of Geodesy Symposia*, vol **133**. Springer, Berlin, Heidelberg
- [11] Younis G, Jäger R and Becker M 2011 Transformation of global spherical harmonic models of the gravity field to a local adjusted spherical cap harmonic model *Arabian Journal of Geosciences*
- [12] Younis G 2013 Regional Gravity Field Modeling with Adjusted Spherical Cap Harmonics in an Integrated Approach. *Schriftenreihe Fachrichtung Geodäsie der Technischen Universität Darmstadt (39)*. Darmstadt. ISBN978-3-935631-28-0 (2013)
- [13] Haines G 1985a Spherical Cap Harmonic Analysis, *Journal of Geophysical Research*, Vol. **90** No. B3.
- [14] Haines G 1985b Spherical Cap Harmonic Analysis of Geomagnetic Secular Variation over Canada 1060-1983, *Journal of Geophysical Research*, Vol. **90** No. B14.
- [15] Haines G 1988 Computer programs for Spherical Cap Harmonic Analysis of Potential and General Fields, *Computer & Geosciences*, Vol. **14**, No. 4.

- [16] De Santis A and Torta J 1997 Spherical Cap Harmonic Analysis: a comment on its proper use for local gravity field representation, *Journal of Geodesy*, Vol. **71**, 1997
- [17] De Santis A, Torta J M and Lowes F J 1999 Spherical Cap Harmonics Revisited and their Relationship to Ordinary Spherical Harmonics *Phys. Chem. Earth (A)*, Vol. **24**, No. 11-12, pp 935 – 941
- [18] De Santis A 1991 Translated origin Spherical Cap Harmonic analysis, *Geophysical Journal International* **106**, 253-263
- [19] Jekeli C 1999 An analysis of vertical deflections derived from high-degree spherical harmonic models, *Journal of Geodesy*, vol. **73**, pp 10-22.
- [20] Torge W 2001 *Geodesy: Third completely revised and extended edition*, Walter de Gruyter, Berlin, New-York
- [21] Vaniček P 1976 *Physical Geodesy, Lecture notes* No. 43, University of New Brunswick